ELSEVIER

Journal of Physics and Chemistry of Solids 61 (2000) 391–396

JOURNAL OF PHYSICS AND CHEMISTRY OF SOLIDS

www.elsevier.nl/locate/jpcs

Correlation and band structure effects in the electronic energy loss spectra of Al: an experimental perspective

B.C. Larson[a,*], J.Z. Tischler[a], A. Fleszar[b], A.G. Eguiluz[c]

[a]*Solid State Division, Oak Ridge National Laboratory, Building 3025, PO Box 2008, Oak Ridge, TN 37831-6030, USA*
[b]*Physikalisches Institut, Universität Würzburg, Am Hubland, 97074 Würzburg, Germany*
[c]*Department of Physics and Astronomy, The University of Tennessee, Knoxville, TN 94551, USA*

Abstract

Inelastic X-ray scattering measurements in aluminum are analyzed using first principles dynamical density response calculations including band structure. Band structure effects are shown to be important; significant effects include shifts of spectral features to lower energies and the presence of high-energy tails, in addition to the much discussed energy gaps and zone-boundary collective states. These non-jellium characteristics must be considered in investigating exchange and correlation effects in simple metals. Published by Elsevier Science Ltd.

Keywords: Band structure

Understanding electronic interactions and correlations is central to obtaining a full description of condensed matter physics. Long-range Coulomb effects are well understood within the mean-field random phase approximation (RPA), but, short-range exchange-correlation (xc) effects have been difficult to handle and descriptions have relied heavily on local density approximations (LDA). The jellium model, described in terms of the Lindhard dielectric function, is often used as a starting point for consideration of the dynamical response of the electronic system for nearly free electron metals. On the other hand, it has long been appreciated that the impact of the ion-core lattice must be taken into account in analyzing energy loss spectra, even for materials with weak pseudopotentials.

The dielectric matrix response for an electronic system with a periodic array of positive ions has been considered by Adler [1], Wiser [2] and, Reiter and Saslow [3]. Foo and Hopfield [4] and later Sturm and Oliveira [5], called attention to the dielectric response to energy gaps at Brillouin zone boundaries and showed that the impact of such gaps on energy loss spectra is the generation zone-boundary collective state (ZBCS) resonances. Singhal [6] compared ZBCS predicted by dynamical response calculations with (small wave vector) electron scattering results. Schülke et al. [7–12] called attention to the presence of band structure induced energy shifts, gaps and high energy tails in Be, and later led to the development of detailed X-ray investigations of electronic loss spectra in metals through the use of the synchrotron X-ray scattering. Platzman and Eisenberger [13] and Eisenberger et al. [14] related periodic ion effects to early X-ray measurements of inelastic scattering in the plasmon regime and later in the single particle behavior [15].

The experimental work of Schülke et al. [7–12] on Be, Li, Al and Si considered the double peak and dispersing features in the loss spectra in relation to band structure effects, and recently the impact of melting on loss spectra has been studied by Hill et al. [16] and Sternemann et al. [17]. On the theoretical side, Quong and Eguiluz [18], Fleszar et al. [19] and Maddocks et al. [20] showed the importance of band structure effects in low symmetry as well as high symmetry directions, and concluded, in particular, that band structure induced gaps give rise to dips (or a double peak structure) in aluminum. Larson et al. [21] showed that a detailed description of the inelastic scattering cross-section for Al could be achieved for all wave vectors using dynamical response calculations in conjunction with an empirical Hubbard-like local-field factor (LFF).

In this paper we compare the measured energy loss spectra for aluminum with first principles dynamical response calculations, including band structure and local field effects

* Corresponding author. Tel.: + 1-423-574-5506; fax: + 1-423-574-4143.

E-mail address: bcl@ornl.gov (B.C. Larson).

0022-3697/00/$ - see front matter. Published by Elsevier Science Ltd.
PII: S0022-3697(99)00323-6

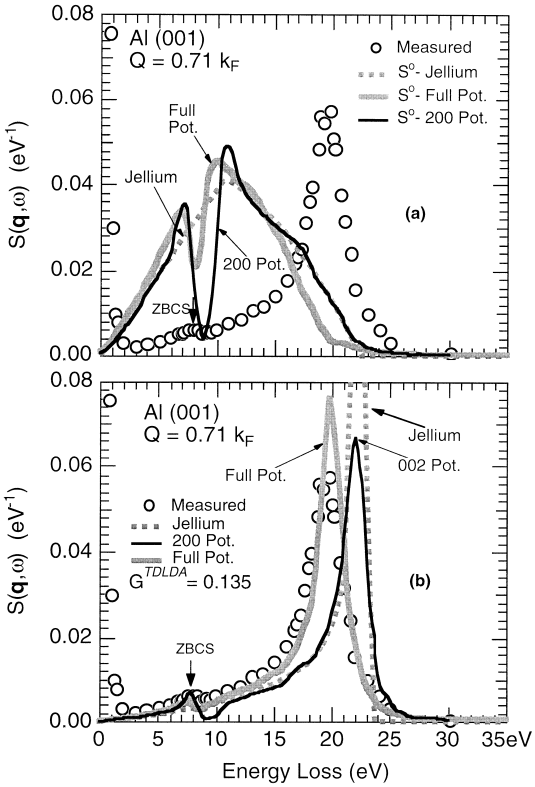

Fig. 1. (a) Measurements of $S(\mathbf{q},\omega)$ for Al at $0.71k_F$ together with $S^0(\mathbf{q},\omega)$ for jellium (dotted), first principles calculations (crystal) with (002) Fourier components of the pseudopotential only (thin-solid), and the full pseudopotential (thick-solid); and (b) measurements and calculations of $S(\mathbf{q},\omega)$ with the above notation and the TDLDA $G(0.71k_F,\omega) = 0.135$.

within the time-dependent extension of the local density approximation [22] (TDLDA). The results emphasize the presence of a band structure induced spectral shift to lower energies and the existence of high-energy tails, in addition to zone-boundary gaps and collective states, all noted qualitatively in relation to Compton scattering 30 years ago [7]. In contrast to the orientation dependence of ZBCS, the spectral shift to lower energies and the high energy tails appear in all directions and for all wave vectors, underscoring the importance of considering the full band structure in analyzing energy loss spectra in terms of xc effects.

Measurements of the dynamical structure factor, $S(\mathbf{q},\omega)$, as a function of the scattered wave vector $\mathbf{q}$ and energy loss ω using inelastic X-ray scattering provide direct information on electronic correlations. $S(\mathbf{q},\omega)$ is related to the dielectric properties of materials through the imaginary part of the inverse dielectric function by [12]

$$S(\mathbf{q},\omega) = -(\hbar\mathbf{q}^2/4\pi^2e^2n)\mathrm{Im}[\varepsilon(\mathbf{q},\omega)]^{-1}_{g=0,g'=0} \quad (1)$$

where

$$\varepsilon(\mathbf{q},\omega) = \{1 - v_{\mathbf{q}}\chi^0(\mathbf{q},\omega)[1 + v_{\mathbf{q}}G(\mathbf{q},\omega)\chi^0(\mathbf{q},\omega)]^{-1}\} \quad (2)$$

is the (matrix) dielectric function, n is the electron density, $\chi^0(\mathbf{q},\omega)$ is the non-interacting polarizability [19], $v_{\mathbf{q}}$ is the Coulomb potential, and $G(\mathbf{q},\omega)$ represents a Hubbard-like LFF to account for short-range xc effects [21]. In general, each of the terms in $\varepsilon(\mathbf{q},\omega)$ is understood to be a matrix in the gg' reciprocal lattice vector representation. Eq. (1) provides a means for direct comparison of first principles calculations of the dynamical structure factor (including band structure and local-field corrections within the TDLDA framework [22]) with experimental measurements of $S(\mathbf{q},\omega)$. For later reference, we define a non-interacting dynamical structure factor, $S^0(\mathbf{q},\omega)$, which (in atomic units; inverse energy) is given by

$$S^0(\mathbf{q},\omega) = -(1/n\pi)\mathrm{Im}\,\chi^0(\mathbf{q},\omega) \quad (3)$$

Inelastic X-ray scattering measurements were made using the X21 beam line at the National Synchrotron Light Source (NSLS) [23]. The measurements were performed using 10 keV incident X-rays and an energy resolution of ~0.75 eV. Aluminum single crystals with ⟨001⟩ and ⟨013⟩ surface normals were used and the scattering was performed in the symmetric Bragg geometry. The scattered X-rays were energy analyzed using a spherically bent Ge analyzer located 1 m from the sample in connection with a low noise, avalanche photo-diode X-ray detector. The data for all wave vectors were reduced to an absolute scale by applying the f sum-rule to measurements made at a wave vector of $1k_F$, for which the entire loss spectrum falls well below the excitation of the (72 eV) $2p$ core level of Al.

Fig. 1 compares inelastic X-ray scattering measurements for Al in the [001] direction at $0.71k_F$ with first principles dynamical response calculations and with the jellium response. The first principles calculations were made for the actual pseudopotential for Al, and also for the case of only the (002) Fourier coefficient of the pseudopotential. The computations were performed as discussed in previous work [19], typically using Troullier–Martins non-local, norm-conserving pseudopotentials with a cutoff of 12 Ryd, corresponding to ~70–80 bands. The experimental measurements in Fig.1(a) and (b), show the presence of a relatively weak zone-boundary collective state at ~8 eV, as a result of final states falling on the [001] zone boundary, and they show the broad plasmon line at ~19 eV. As was shown in earlier studies [18], the full band structure calculations (with the TDLDA $G(\mathbf{q},\omega)$) provide a rather good description of the plasmon energy; we show here that the calculations account for the ZBCS at 8 eV and the overall shape of the loss spectrum as well. It is interesting to note that the calculation including only the (002) Fourier coefficient of the pseudopotential contains the full effect of the ZBCS, but the plasmon position for this calculation is nearly jellium like. This indicates the importance of considering

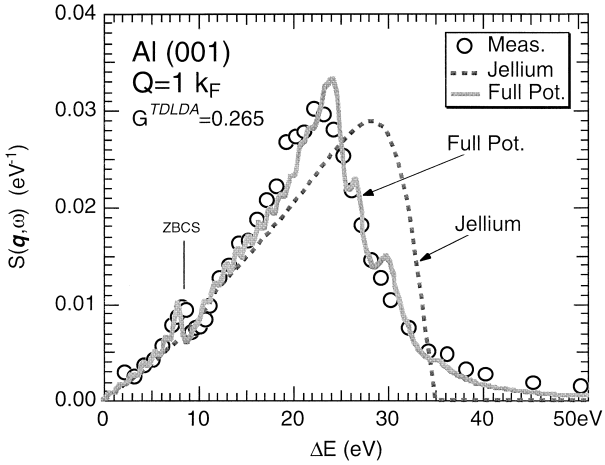

Fig. 2. Measurements of $S(\mathbf{q},\omega)$ for $1k_F$ together with calculations of $S(\mathbf{q},\omega)$ for jellium (dotted) and first principles calculations including the full pseudopotential (solid); both calculations use the TDLDA $G(1k_F,\omega) = 0.265$.

the full band structure and the inadequacy of simple two-band models for quantitative investigations.

Although $S(\mathbf{q},\omega)$ is dominated by the oscillator strength of the plasmons for wave vectors below the onset of Landau damping, the non-interacting response $S^0 0\mathbf{q},\omega) \propto \mathrm{Im}\chi^0(\mathbf{q},\omega)$ in Eq. (3) (where $G(\mathbf{q},\omega) = 1$ and Coulomb and local-field interactions cancel) provides important insight into the nature of the overall effect of band structure on energy loss spectra of simple metals. Comparing the shape of calculations including band structure with the (shark fin) shape of $S^0(\mathbf{q},\omega)$ for jellium, we note the large dip near 8 eV resulting from the gap at this energy on the [001] zone boundary. When combined with the accompanying resonance structure of the Re $\chi^0(\mathbf{q},\omega)$ at the gap (as

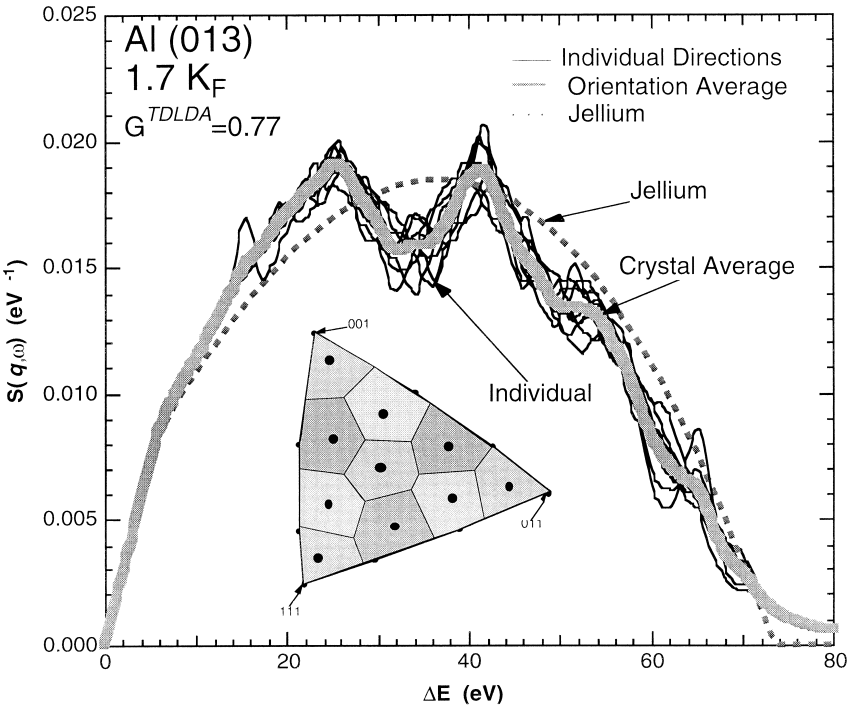

Fig. 3. Calculations of $S(\mathbf{q},\omega)$ at $1.7k_F$ for the ten directions indicated by solid circles within the 111–011–001 triangle (thin solid lines); the thick solid line represents the average over the ten orientations; the dotted line represents a jellium calculation; all calculations use the TDLDA $G(1.7k_F,\omega) = 0.77$.

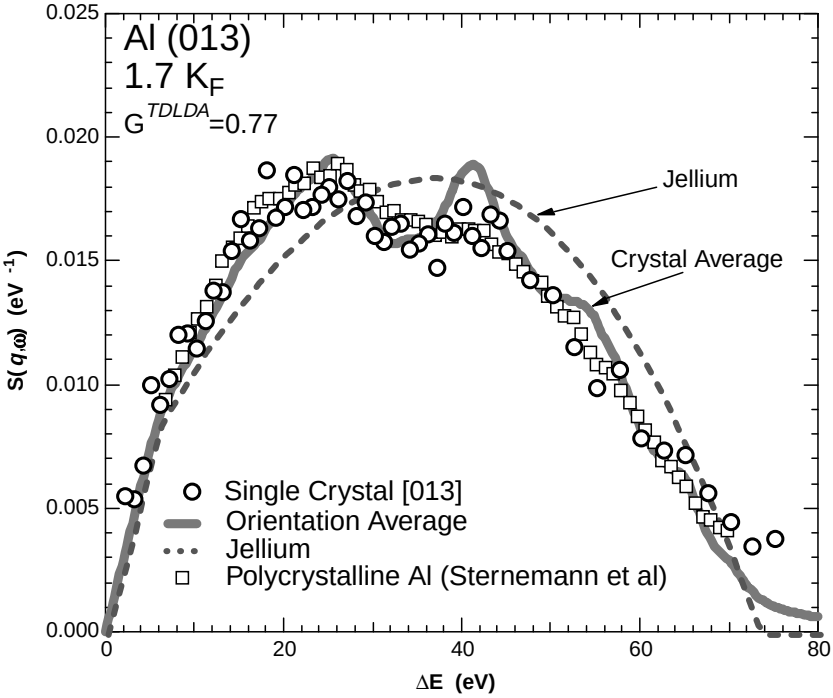

Fig. 4. Orientation-averaged (thick solid line) and jellium (dotted) calculations of $S(\mathbf{q},\omega)$ together with measurements along the [013] direction (open circles) and polycrystalline measurements from Ref. [12] (open squares); the calculations are as in Fig. 3.

discussed in detail by Foo and Hopfield [4] and Sturm and Oliviera [5]) both the positive resonance and the dip in the measured intensity at 8 eV are understood as a classic ZBCS. Gaps on other zone-boundaries such as the [002] to be discussed later are of much larger significance.

We emphasize, though, that there are two additional features introduced into $S^0(\mathbf{q},\omega)$ by the band structure that are actually more general than the presence of the zone boundary collective states. They are: (1) the overall shift of the spectral weight to lower energies, as a result of the non-homogeneous potential; and (2) the high energy tails on $S^0(\mathbf{q},\omega)$ resulting from the Bloch states (rather than plane wave jellium states) for electrons propagating in the positive ion lattice. As already discussed above, the ⟨001⟩ zone boundary is alone responsible for the presence of the gap at 8 eV, while the ⟨002⟩ Fourier coefficient of the pseudopotential accounts for only a small part of the plasmon energy shift. Similarly, we see that the ⟨002⟩ Fourier coefficient accounts for only a small part of the erosion of the high-energy side of $S^0(\mathbf{q},\omega)$ and a small part of the spectral shift toward lower energies. Even the inclusion of the ⟨111⟩, ⟨220⟩, ⟨311⟩, ⟨222⟩ and ⟨400⟩ pseudopotential Fourier components in addition to the ⟨002⟩ component does not account for all of the shift.

Fig. 2 shows results for $q = 1k_F$ in which a more pronounced ZBCS and a stronger non-jellium high-energy tail are present. As was the case for $0.71k_F$, the jellium response for $1k_F$ peaks at a significantly larger energy than observed experimentally. Although not plotted, the spectrum of $S^0(\mathbf{q},\omega)$ for $1k_F$ is shifted to lower energies and contains a significant high energy tail compared to the jellium result. The close correspondence of the TDLDA first principles $S(\mathbf{q},\omega)$ calculations with the measured scattering distributions for the low q values, in both Figs. 1 and 2, leads to the general conclusion that the TDLDA $G(\mathbf{q},\omega)$ represents an adequate approximation for wave vectors $\sim k_F$—as concluded by Larson et al. [21] previously.

Turning to the larger wave vector regime, Fig. 3 considers the $q = 1.7k_F$ case for aluminum. This region continues to draw both theoretical and experimental attention as a result of a ubiquitous dip (or double-peak) structure that is observed in single crystals, and which persists for polycrystals and is even evident in the liquid state [16,17]. As mentioned earlier, first principles calculations [19,20] report a dip structure in the ~32 eV region for the relatively low-symmetry [013] direction. We show in Fig. 3 that first principles calculations for Al contain a dip in this energy range for *all* directions. The thin solid lines in Fig. 3 were made for the 10 directions distributed within the (001)–(111)–(011) triangle in the inset; the thick line in Fig. 3 represents the average of the 10 directions. This average spectrum is shown in Fig. 4 to be in remarkably good agreement with the (open circles) measurements made at $1.7k_F$ in the [013] direction. Also plotted in Fig. 4 are polycrystalline Al measurements published recently by Sternemann et al. [17]. The polycrystalline Al measurements of Sternemann

are in good agreement with the orientation averaged TDLDA calculations, and we note that they are remarkably similar to the measurements in the low symmetry [013] direction.

Of course, the persistence of the large dip in the calculated electronic response near ~32 eV for all directions is not the result of zone boundaries perpendicular to each direction. Neither is it solely the result of the large ($\Delta E \sim$ 6 eV) gap [19] on the [002] zone boundary extending the dip to other directions. Rather, it can be understood in the context of the band structure effects that lead to the well-known gap in the density of states of Al at ~30 eV. The large gap on the [002] zone boundary is a combined result of the sizeable (022) shell Fourier components (and other shells) as well as the (004) Fourier component of the pseudopotential. The strength apparently stems from the fact that the valence electron final states involved have predominantly *d* character below the gap and *f* character above the gap, neither of which can be fully shielded from the ion potential because of the absence of core electron states with these angular momenta [24–26].

It should be noted that the gap in the density of states is observed in LAPW all-electron calculations [26] as well as pseudopotential calculations for Al, and also that the dips in the calculated response functions are quite insensitive to the choice of pseudopotentials. Moreover, since the geometrical aspects related to zone boundaries, final state symmetries, etc. are handled routinely in the response calculations presented here, the band structure origin of the dips is not in question.

We note the relatively sharper structure in the computations in Figs. 3 and 4 compared to the measurements. This is largely a result of the fact that the first principles response calculations do not include self-energy effects (real or imaginary), although a small damping factor of 0.5 eV has been used to reduce finite k-mesh sampling effects in the large-q calculations and 0.1–0.2 eV for small-q. It is known that the introduction of on-shell self-energy effects (i.e. imaginary part) tends to reduce sharp structures in the response, and even leads to a double-peak like structure in the jellium response at large wave vectors (see discussions by Sterneman et al. [17] recently and Schülke et al. [11]). A discussion of self-energy effects is outside the scope of this paper; we comment, though, that on-shell self-energy (i.e. lifetime only) corrections lack justification [17,27,28], and that a proper first principles calculation needs both the real and imaginary parts introduced self-consistently within the band structure calculations.

We note in Fig. 3 that the variations in the calculated spectra for the individual directions are far overshadowed by the overall similarity in the shape of the calculated spectra, and we comment that the TDLDA $G(\mathbf{q},\omega) = 0.77$ is close enough to unity for $1.7k_F$, that $S(\mathbf{q},\omega)$ is similar in shape to $S^0(\mathbf{q},\omega)$. We note also that the change in shape of the crystal response relative to that for jellium is quite analogous to that discussed for $S^0(\mathbf{q},\omega)$ for a wave vector of $0.71k_F$ in Fig. 1. In fact, it appears that the inhomogeneous nature of the positive ion-core lattice induces a shape in $S^0(\mathbf{q},\omega)$ that is "universal" for small as well as large wave vectors. We emphasize that it is this departure from jellium (i.e. shift to lower spectral energy and the high energy tails) that is primarily responsible for the direct correspondence of the TDLDA response calculations with the experimental $S(\mathbf{q},\omega)$ measurements at all wave vectors.

Therefore, the lack of a significant change in the shape of energy loss spectra toward a more jellium-like shape upon melting [16,17] (e.g. toward higher energies and/or to a sharper high energy cut-off), can be regarded as evidence that the local order [29,30] within these metallic liquids maintains the essential electronic structural aspects of the lattice. This interpretation was suggested by early NMR measurements [29] on liquid metals, and is consistent with the interpretation reached by Hill et al. [16] in regard to inelastic scattering measurements on liquid Na and Li. We believe the results of Sternemann et al. [17] on liquid Al fall within this interpretation as well.

Acknowledgements

Helpful discussions with W. Ku are acknowledged. This work was supported by the US DOE under Contract No. DE-AC05-96OR22464 with Lockheed–Martin Energy Research, Inc. The measurements were performed on the X21 beam line at the National Synchrotron Light Source operated by Brookhaven National Laboratory for the Department of Energy. A.G.E. was supported by NSF Grant No. DMR-9634502 and the National Energy Research Supercomputer Center.

References

[1] S.L. Adler, Phys. Rev. 126 (1962) 413.
[2] N. Wiser, Phys. Rev. 129 (1963) 62.
[3] W.M. Saslow, G.F. Reiter, Phys. Rev. B 7 (1973) 2995.
[4] E.N. Foo, J.J. Hopfield, Phys. Rev. 173 (1968) 635.
[5] K. Sturm, L.E. Oliveira, Phys. Rev. B 30 (1984) 4351.
[6] S.P. Singhal, Phys. Rev. 14 (1976) 2352.
[7] W. Schülke, U. Berg, Phys. Status Solidi 23 (1967) K87.
[8] H. Nagasawa, S. Mourikis, Phys. Rev. Lett. 52 (1984) 2065.
[9] W. Schülke, H. Nagasawa, S. Mourikis, P. Lanzki, Phys. Rev. B 33 (1986) 6744.
[10] W. Schülke, H. Nagasawa, S. Mourikis, A. Kaprolat, Phys. Rev. B 40 (1989) 12 215.
[11] W. Schülke, H. Schulte-Schrepping, J.R. Schmitz, Phys. Rev. B 47 (1993) 12 426.
[12] W. Schülke, J.R. Schmitz, H. Schulte-Schrepping, A. Kaprolat, Phys. Rev. B 52 (1995) 11 721.
[13] P.M. Platzman, P. Eisenberger, Phys. Rev. Lett. 33 (1974) 152.
[14] P. Eisenberger, P.M. Platzman, K.C. Pandy, Phys. Rev. Lett. 31 (1975) 311.
[15] P.M. Platzman et al., Phys. Rev. B 46 (1992) 12 943.

[16] J.P. Hill, C.-C Kao, W.A.C. Caliebe, D. Gibbs, J.B. Hastings, Phys. Rev. Lett. 77 (1996) 3665.
[17] C. Sternemann, A. Kaprolat, W. Schülke, Phys. Rev. B 57 (1998) 622.
[18] A.A. Quong, A.G. Eguiluz, Phys. Rev. Lett. 70 (1993) 3955.
[19] A. Fleszar, A.A. Quong, A.G. Eguiluz, Phys. Rev. Lett. 74 (1995) 590.
[20] N.E. Maddocks, R.W. Godby, R.J. Needs, Europhys. Lett. 27 (1994) 681.
[21] B.C. Larson, J.Z. Tischler, E.D. Isaacs, P. Zschack, A. Fleszar, E.G. Eguiluz, Phys. Rev. Lett. 77 (1996) 1346.
[22] A. Zangwill, P. Soven, Phys. Rev. A 21 (1980) 1561.
[23] W. Caliebe, C.-C. Kao, M. Krisch, T. Oversluizen, P. Montanez, J.B. Hastings, in: E. Fontes (Ed.), Synchrotron Radiation Instrumentation: Tenth US National Conference, American Institute of Physics, New York, 1997, p. 6.
[24] A.P. Sutton, Electronic Structure of Materials, Clarendon Press, Oxford, 1993, p. 153.
[25] H.J. Levinson, F. Greuter, E.W. Plummer, Phys. Rev. B 27 (1983) 727.
[26] K. Wei, private communication of WIEN95 LAPW all-electron calculations.
[27] T.K. Ng, G. Dabrowski, Phys. Rev. 33 (1986) 5358.
[28] G. Niklasson, Solid State Commun. 54 (1985) 665.
[29] W.D. Knight, A.G. Berger, Ann. Phys. 8 (1959) 173.
[30] M.S. Zei, R. Hoseman, Phys. Rev. B 18 (1978) 6560.